

A 5 TESLA SUPERCONDUCTING MAGNET AND CRYOSTATS  
FOR AN EPR / FMR SPECTROMETER

E.M.C.M. Reuvekamp, G.J. Gerritsma, H.H.J. ten Kate, L.J.M. van de Klundert

University of Twente  
Department of Applied Physics  
P.O. Box 217, 7500 AE Enschede,  
the Netherlands.

Abstract

An Electron Paramagnetic Resonance Ferromagnetic Resonance (EPR/FMR) spectrometer, using Ka-band (26.5-40 GHz) and U-band (40-60 GHz), is built for resonance measurements on among others large magnetic thin films. It has the following features:

- a) a superconducting magnet with a homogeneous (< 90 ppm in sphere  $\phi = 20$  mm) magnetic field up to 5 tesla.
- b) a free rotation of magnet field around the sample.
- c) a broad temperature range of the EPR/FMR sample (4 to 300 K).

This paper concerns the cryogenic part of the spectrometer, consisting of two cryostats.

Firstly, there is a cryostat having a room temperature vertical inlet tube, that gives access to the centre of the magnet. This cryostat can be rotated around the central axis of the inlet tube and enables rotation of the magnetic field around a fixed sample, placed in the centre of the magnet. To reduce liquid helium evaporation special care is taken in the construction of the cryostat, by applying helium gas heat exchangers for instance. This cryostat contains a superconducting Helmholtz-like coil (up to 5 tesla at the centre). Secondly there is a flow cryostat placed freely in the inlet tube of the first cryostat. This cryostat is used to cool the EPR/FMR sample.

Special attention is paid to the construction of both cryostats, as well as to the design-calculations and construction of the superconducting magnet coil. The calculations are compared with experimental data.

Introduction

In our laboratory the demand arose for a new EPR/ FMR spectrometer, along with an already present 3 tesla X-band (8.2-12.4 GHz) spectrometer. The new spectrometer had to meet the following specifications:

- the microwave frequencies to be used are in the Ka- (26.5-40 GHz) and the U-band (40-60 GHz).
- the direction of the magnetic field at the EPR/FMR sample should be adjustable between  $0^\circ$  and  $180^\circ$ .
- the possibility to do EPR/FMR measurements on large samples, up to a length of 20 mm, such as thin magnetic films.
- the sample temperature has to be controllable from room temperature down to about 4 K.

Simple EPR/FMR theory must be applied to translate these needs into the requirements for the new spectrometer.

The EPR/FMR measuring technique gives information, on a microscopic scale, about the atomic structure of the sample. If a sample with non-zero resultant electron-spin is placed in a magnetic field, its energy levels will split up according to the Zeeman-effect. Transitions between these Zeeman-levels can be induced by irradiating with microwaves. These transitions are detected as absorption of microwave power. The connection between the microwave frequency and the applied magnetic field in case of absorption follows from conservation of energy:

$$h\nu = \mu_B \bar{g} \bar{S} \cdot \bar{B}, \quad (1)$$

where  $h$  : Planck's constant,  
 $\nu$  : microwave frequency,  
 $\mu_B$  : Bohr's magneton ( $= \frac{eh}{4\pi m}$ ),  
 $\bar{g}$  : spectroscopic splitting factor (a tensor),  
 $\bar{S}$  : electron-spin vector,  
 $\bar{B}$  : applied magnetic field.

The g-factor contains information about the atomic structure and is in principle anisotropic (a tensor) and can be temperature dependent. Substitution of the values of the physical constants and the free electron approximation,  $g=2.0023$  and  $|\bar{S}| = .5$ , shows that the microwave frequency is:

$$\nu \text{ (GHz)} = 14.0 |\bar{B}|. \quad (2)$$

Thus with fields around a few tesla, that can be achieved in the laboratory, the required radiation will lie in the microwave region.

In the spectrometer the microwave frequency is kept constant, and the magnetic field is swept. Absorption is measured as a function of the magnetic field, so the g-factor(s) and thus information about the atomic structure can be determined. Further information is gained from the shape of the absorption peak. Line widths at microwave frequencies vary from a few gauss (very narrow) to several hundred gauss (broad). This puts demands upon the homogeneity of the magnetic field at the sample.

According to (1), assuming a microwave frequency independent line width, higher microwave frequencies give better resolution of the absorption as a function of the magnetic field. This is the main reason for using higher microwave frequencies. From equation (2) it follows that for microwave frequencies of 60 GHz, a magnetic field of at least 4 tesla should be used. The inhomogeneities of the magnetic field at the sample should be much less than the line width of the microwave absorption peak, otherwise a good measurement of the line shape function is not possible. For our samples this should result in a homogeneity better than 100 ppm. Because the intention was to make measurements on large samples up to 20 mm long, this homogeneity was required in a sphere  $\phi = 20$  mm. In order to study the anisotropy of the g-factor free rotation of the magnetic field of at least  $0^\circ$ - $180^\circ$  was needed. In our case it was considered necessary to rotate the whole magnet with its cryostat and keep the sample fixed, if the sample temperature was to be accurately known during the experiments. To determine the temperature dependence of the g-factor the sample is cooled in a separate flow cryostat. The desired temperature range for our samples is from room temperature down to about 4 K. The flow cryostat is another cryogenic part of the spectrometer, separate from the superconducting magnet and its cryostat, and so will also be discussed separately.

The superconducting coil

A Helmholtz coil-set, outlined in figure 1, has in principle 6 free parameters;  $a_1, a_2, b_1, b_2, N_1, N_2$ , where  $a, b$  are the dimensions of the coil and  $N_1, N_2$  the number of windings in the  $r$ -, respectively,  $z$ -direction. These parameters were determined by using the following starting conditions:

- 1- the magnetic field  $B_z(z=0, r=0) = B_z(z=\pm z_0, r=0)$  for  $z_0 = 12.5$  mm.
- 2- the presence of a radial access to the centre of the magnet determines the coil spacing,  $2b_1 \approx 62.50$  mm.
- 3- the wire diameter,  $d = 0.74$  mm, relates  $a_2$  to  $a_1, N_1$  and  $b_2$  to  $b_1, N_2$ :  
 $N_1 d = (a_2 - a_1)$   
 $N_2 d = (b_2 - b_1)$
- 4- the volume of the coil  $V = (b_2 - b_1) \pi (a_2^2 - a_1^2)$  should be minimal.
- 5- the homogeneity of the  $z$ -component of the field  $B_z$  for  $|z| \leq z_0$  is kept to a minimum and is less than 100 ppm:

$$\frac{B_z(|z| \leq z_0, r=0) - B_z(z=0, r=0)}{B_z(z=0, r=0)} < 10^{-4}$$

- 6- the magnet should fit in the cryostat:  
 $\sqrt{a_2^2 + b_2^2} < 200$  mm.
- 7- the magnetic field at the centre of the magnet must be at least 5 tesla.

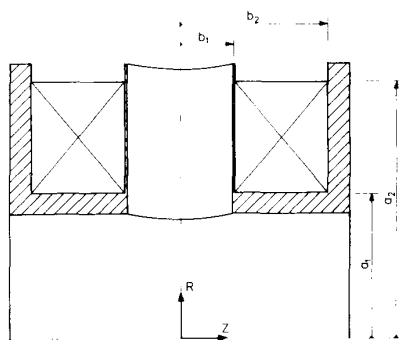


Figure 1: A cross-section of the 5 tesla Helmholtz coil-set, with an Al former.

So there are 8 equations, under which three equalities, for determining 6 parameters. From different designs the one with the parameters presented in table 1 was chosen. The coil bobbin is made from aluminium, and is attached to the bottom of the cryostat.

It follows from  $\text{div } \vec{B} = 0$  and  $\text{rot } \vec{B} = 0$  that the same order of homogeneity holds for the  $B_z$  component in radial and axial directions. From this the conclusion is made that a homogeneity  $< 100$  ppm is achieved in a sphere  $\phi = 20$  mm, and not only at the axis  $r=0$ . Measurements of the  $B_z$  component are performed on the  $z$ -axis with a NMR magnetometer. These measurements are presented in figure 2. From this figure it is seen that a homogeneity  $< 100$  ppm is reached on a length  $\Delta z = 29.5$  mm.

Table 1; Parameters of the coil-set.

<p>Conductor :</p> <p>NbTi in copper matrix,                  NbTi/Cu ratio 1:1.8;                  2070 filaments with a diameter 9.0 <math>\mu\text{m}</math>;                  round wire, bare 0.686 mm,                  insulated 0.740 mm;                  Manufacturer MCA;</p>
<p>Coil :</p> <p>dimensions (see figure 1):  <math>a_1 = 8.257 \cdot 10^{-2}</math> m, <math>a_2 = 14.47 \cdot 10^{-2}</math> m;  <math>b_1 = 3.125 \cdot 10^{-2}</math> m, <math>b_2 = 8.225 \cdot 10^{-2}</math> m;                  solenoid wet-wound with Stycast 2850FT;                  inductance <math>L = 19.3</math> H; turns = 11574;                  wire length = 8264 m;                  max. stored energy <math>W_L = 117</math> kJ;                  max. current <math>I = 110</math> A;                  max. sc. current density <math>J_{sc} = 833</math> A/mm<sup>2</sup>;                  max. av. current density <math>J_{av} = 298</math> A/mm<sup>2</sup>;                  ( in metal )                  field ratio <math>B/I = 0.04583</math> T/A;                  metal filling factor = 66.8 %;</p>

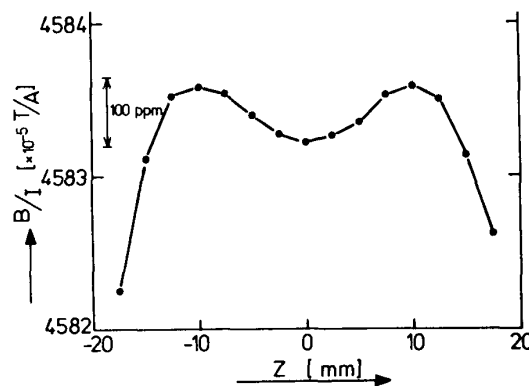


Figure 2; Measured  $B_z$  component on the  $z$ -axis ( $r = 0$ ).

### Protection of the magnet

The maximum temperature in the superconducting wire after a quench, in case of adiabatic heating of the wire is obtained from:

$$\int_{t=0}^{t=\infty} J^2(t) dt = \int_{T=4.2}^{T_f} \frac{\sigma c(T)}{\rho(T)} dT = K(T_f), \quad (3)$$

where  $t$  : time,  
 $J(t)$  : current density,  
 $\sigma$  : mass density,  
 $T$  : temperature,  
 $c(T)$  : specific heat of the wire,  
 $\rho(T)$  : electrical resistivity,  
 $T_f$  : final temperature of the wire,  
 $K$  : thermal load-integral.

If the current decays exponentially, with a decay-time  $\tau$ , and flows almost totally in the copper matrix thereby heating up the total wire (copper matrix and superconducting filaments), equation (3) reduces to:

$$J_{sc}^2(0) \tau = 2 \frac{1-\eta}{\eta^2} K_{Cu}(T_f), \quad (4)$$

where  $J_{sc}(0)$  the initial current density in the sc filaments before a quench,  
 $\tau$  current decay time,  
 $\eta$  sc filling factor  
 (=0.36 for our wire),  
 $K_{Cu}(T_f=100 \text{ K.}) = 8.0 \cdot 10^{16} \text{ A}^2 \text{sm}^{-4}$  [1],  
 $K_{Cu}(T_f=300 \text{ K.}) = 1.4 \cdot 10^{17} \text{ A}^2 \text{sm}^{-4}$  [2].

Measurements performed on a similar superconducting coil by ten Kate et al. [3] showed a  $\tau \approx 1$  s. This means :

$J_{sc}(T_f=300 \text{ K.}) = 1.2 \cdot 10^9 \text{ Am}^{-2}$  and  
 $J_{sc}(T_f=100 \text{ K.}) = 8.9 \cdot 10^8 \text{ Am}^{-2}$ .  
 For our coil  $T_f < \approx 100$  kelvin, because  
 $J_{sc, \max} = 8.35 \cdot 10^8 \text{ Am}^{-2}$ , which was acceptable.  
 Training of the maximum current of about 10% was observed. The first quench was measured at  $I = 98.9$  A (4.53 tesla), the second at  $I = 109.1$  A (5.00 tesla).

### The magnet cryostat

The designed cryostat, containing the superconducting coil, has the following features:

- the whole cryostat, including the superconducting coil can be freely rotated,
- the presence of a room temperature vertical access, bore  $\phi = 40$  mm, to the test volume at the centre of the magnet,
- heat exchangers, giving off heat from the radiation shields to the evaporated cold helium gas, minimize heat leak,
- the magnet current leads ( $I_{\max} = 110$  A) are of the helium gas counter-flow type.

With this design the evaporation rate of liquid helium is determined at  $1.0 \text{ lh}^{-1}$  ( $I=0$  A) and at  $1.11 \text{ lh}^{-1}$  ( $I=77$  A). The helium gas flow outside the cryostat at room temperature was measured and a cold gas ( $T = 4.2\text{K.}$ ) correction was made for the volume of evaporated liquid helium. This evaporation rate is small enough to have intervals between refills of about 1 day, which is quite acceptable. A cross-section of the cryostat is presented in figure 3. The cryostat bearing, vertical access to the test volume and the helium gas heat exchangers are shown.

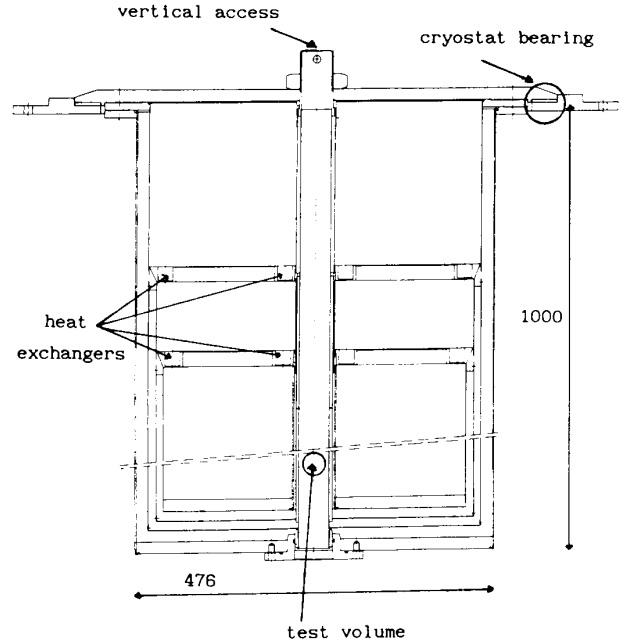


Figure 3; The cross-section of the magnet cryostat.

The helium gas heat exchangers are made of stacked copper small-mesh wire-netting in good thermal contact with the radiation shields. The counter flow current leads are optimized according to Wilson's approach [4]. This approach states that optimum current leads dimensions are given by:

$$\frac{I_0 X_{z0}}{A_0} = \gamma \text{ (material dependent)}, \quad (5)$$

where  $I_0$  : optimized current,  
 $X_{z0}$ : optimum length of lead between  $T = 300 \text{ K.}$  and  $T_{He} = 4.2 \text{ K.}$ ,  
 $A_0$  : optimized cross-area,  
 $\gamma$  : material dependent constant  
 (in our case high conductivity copper;  $\gamma = 2.6 \cdot 10^7 \text{ Am}^{-1}$ ).

For our current leads  $X_{z0} = 0.6$  m,  $I_0 = 100$  A, so it follows that  $A_0 = 2.3 \text{ mm}^2$ . The current leads are made of copper foil to achieve a large perimeter and thus a better heat transfer efficiency from the current lead to the cooling helium gas. The dimensions chosen are slightly oversized,  $10.0 \cdot 0.3$  mm, for safety reasons. The calculated evaporation rate of liquid helium, for the two current leads only, is  $0.29 \text{ lh}^{-1}$  for optimum current ( $I=100$  A), and  $0.19 \text{ lh}^{-1}$  for zero current ( $I=0$  A). The difference between these two values is about the same as the measured difference between loaded ( $I=77$  A) and unloaded ( $I=0$  A) conditions. The largest heat leak is expected to be caused by the room temperature vertical access, because of the lack of a second radiation shield round this access.

A passive quench protection has been chosen. This is acceptable because the maximum final temperature  $T_f$  is far lower than 300 kelvin. Pressure reliefs in the radiation shields in the inner cryostat and in the top plate are added to handle the helium boil-off after a quench safely. A rough approximation of the gas flow by the helium boil-off can be made by calculating the heat flux into the liquid helium. Using the film-boiling model of Ogata and Nakayama [5] this heat flux was roughly determined as 2.5 kW, giving a boil-off of about  $1 \text{ ls}^{-1}$  liquid helium. This value agreed with the measured evaporation rates after the first two quenches. After these quenches during test runs, burn out of the superconducting coil did not occur and the helium gas was blown off without complications.

#### The flow cryostat

The flow cryostat contains two heat exchangers in the lower inner part that enable cooling of the sample. The sample is mounted in a microwave resonance cavity under the lowest heat exchanger (he1). A cross-section of the flow cryostat is presented in figure 4. A cryogen (helium or nitrogen) flows through both heat exchangers, thereby absorbing up heat and so cooling the lower part of the inner cryostat. Heat insulation is obtained by a vacuum space with one highly polished gold plated copper radiation shield. This radiation shield has good thermal conduction to the upper heat exchanger (he2).

From measurements performed on a prototype the conclusion is that temperatures down to 5 kelvin were obtainable, although the coolant flow-resistance was rather high. In the definite version, which is in progress, the supply and outlet pipes of the coolant are enlarged. By this sufficient flow to cool down below 5 kelvin can be obtained. It is expected that by reducing the pressure at the outlet, the sample temperature can be lowered below 4.2 kelvin.

A normal Ka-band waveguide, WR-28, of inside dimensions  $0.711 \times 0.356 \text{ cm}$  was used. To lower the heat leak, Invar (Nilo 36) was chosen. In the case of using U-band microwaves we have to work oversized. We use a cylindrical resonance cavity, operated in  $TE_{011}$  mode (Ka-band) or  $TE_{012}$  mode (U-band). Because the sample has a bad heat contact with the heat exchanger in this cavity, we have to use helium contact gas for better thermal contact.

Temperature stabilization is obtained by the large thermal mass of the heat exchangers, by controlling the flow of coolant and by an electrical heater mounted on the lower heat exchanger (he1). The temperature is measured at the lower heat exchanger, using a thermocouple and carbon resistor thermometers.

The controls for tuning the resonance cavity to critical coupling can be operated from the outside, at the top of the flow cryostat. The sample is also inserted and, if desired, rotated from the outside of the flow cryostat.

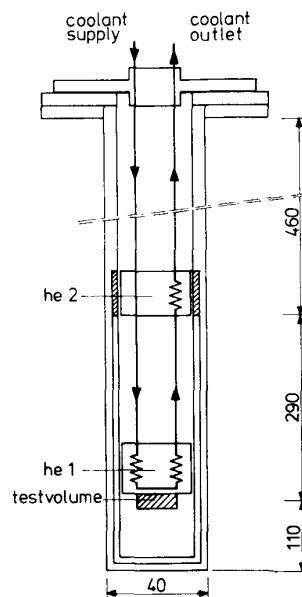


Figure 4; The cross-section of the flow cryostat.

#### Conclusions

A 5 tesla EPR/FMR spectrometer, with a superconducting magnet, was built for Ka- and U-band microwaves. It appeared to be possible to design and construct a superconducting magnet according to the following specifications: the homogeneity  $< 100 \text{ ppm}$  in sphere  $\phi=20 \text{ mm}$ , and  $B_{\text{max}} \geq 5 \text{ tesla}$ .

The magnetic field at the sample is freely adjustable by either rotating the magnet with its cryostat, or rotating the sample. The sample temperature is controllable from room temperature down to below 4 kelvin, using a separate special flow cryostat.

#### References

- [1] A. Ulbricht, Theoretische und experimentelle Untersuchungen über die Eigenschaften ...etc. (40MW, 47 kV switch), Thesis ETHZ (Diss. ETH 6194) 1978, ch. 3, pp.12.
- [2] H.H.J. ten Kate, Superconducting rectifiers, Thesis THT, 1984, ch. 9, pp. 170-173.
- [3] H.H.J. ten Kate et al., "Normal zone propagation in a wet-wound thick solenoid", Proceedings of the 9<sup>th</sup> International Conference on Magnet Technology, 1985, pp. 588-591.
- [4] M.N. Wilson, Superconducting magnets, Monographs on cryogenics, Clarendon Press Oxford 1983, ch. 11, pp. 256-271.
- [5] H. Ogata and W. Nakayama, "Heat transfer to boiling helium from machined and chemically treated copper surfaces", Advances in cryogenic engineering, Vol.27 (1981), pp. 309-317.